Supplementary Information for

Partial oxidation of the absorber layer reduces charge carrier recombination in antimony sulfide solar cells

Karl C. Gödel, Bart Roose, Aditya Sadhanala, Yana Vaynzof,
Sandeep K. Pathak, Ullrich Steiner*

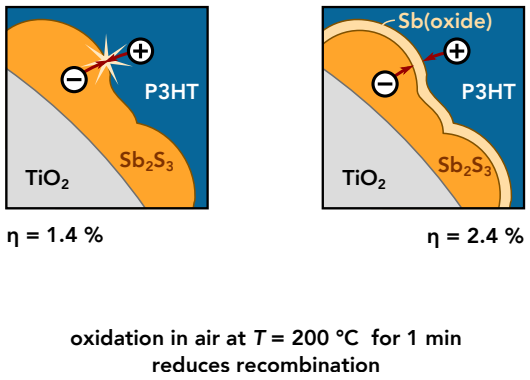

Figure S1: TOC: Surface oxidation by a controlled heat treatment in air leads to improved Sb_2S_3 sensitized solar cells by the reduction in charge carrier recombination.

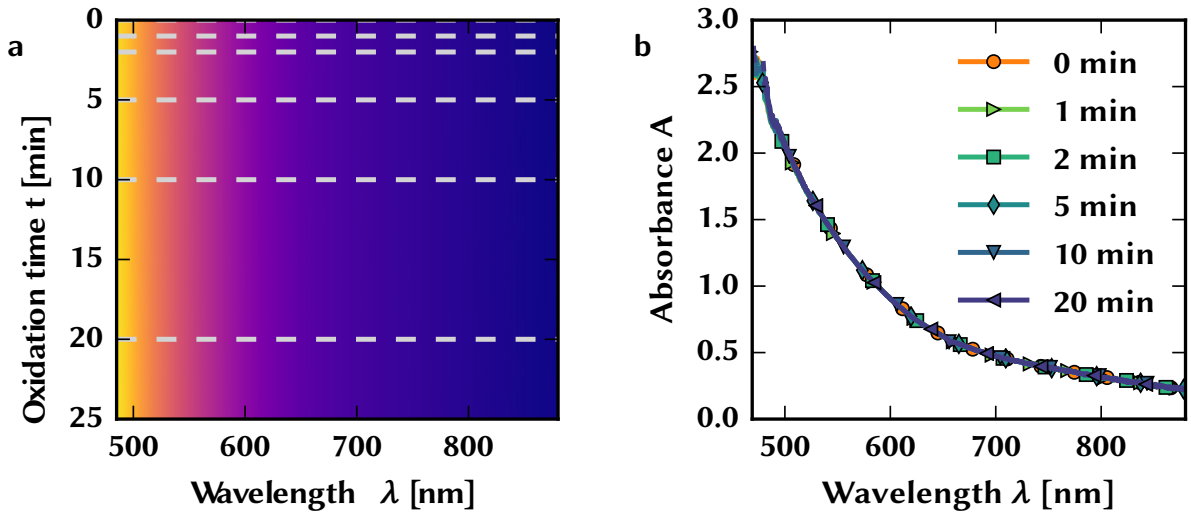

Figure S2: In situ absorbance measurement of oxidizing antimony sulfide. (a) A 2D map of the measured spectrum with oxidation time. The absorbance value is colour coded. (b) Absorbance spectra for six different oxidation times (dashed lines in (a)).

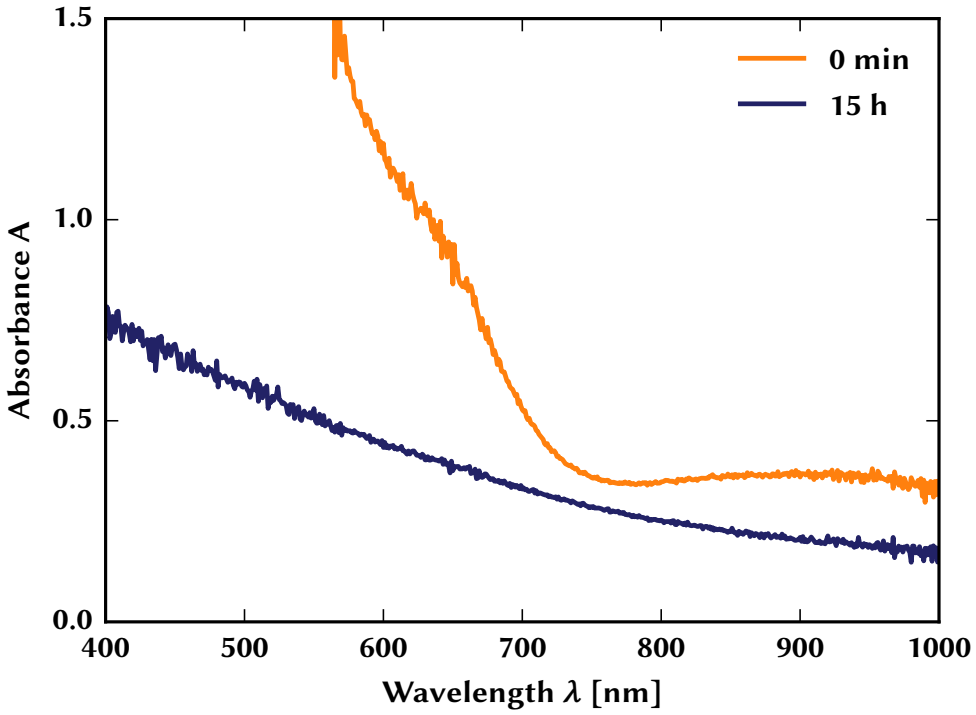

Figure S3: A long oxidation period of 15 hours at 200 °C leads to the deterioration of the absorbance spectrum of Sb_2S_3. The sample changes colour from dark brown to pale white.

For extremely long oxidation periods (15 h), the clear onset corresponding to the band-gap of crystalline antimony sulfide disappeared and the overall absorption decreased. The oxidisation of the sample is also observable by eye, the colour changed from dark brown (typical for crystalline Sb_2S_3) to a pale, transparent white.

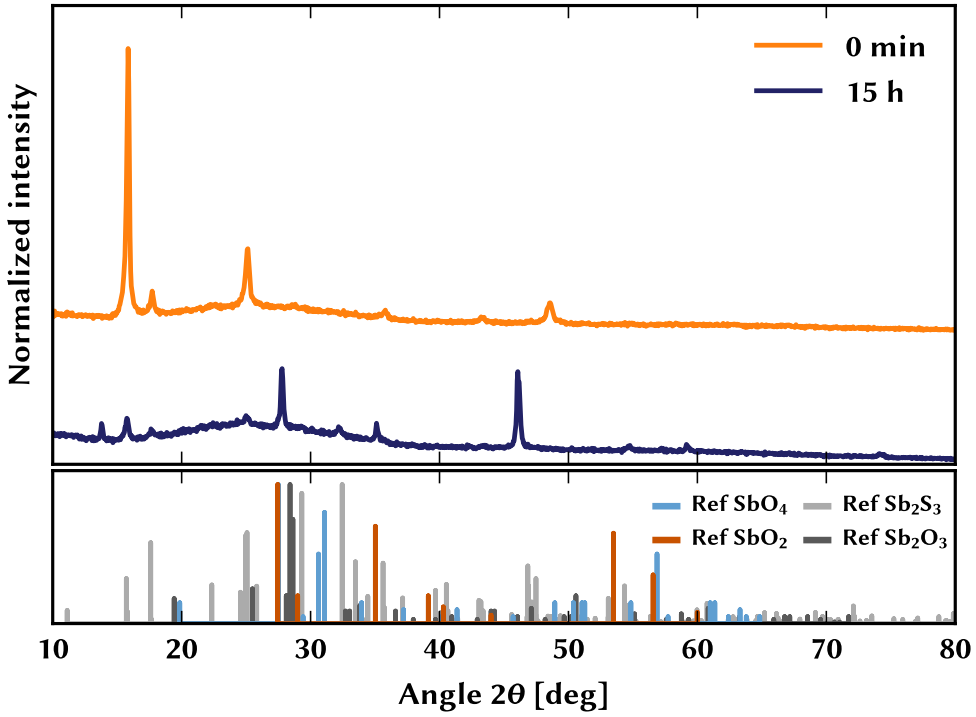

Figure S4: X-ray diffraction pattern of an as annealed antimony sulfide film compared to an oxidized film, which was heated at 200 °C for 15 hours. As a reference, different phases of antimony oxide are shown.

For extremely long oxidation periods, the Sb_2S_3 peaks disappear almost completely, but new peaks appear. Since they cannot be assigned to a single phase of antimony oxide, it is likely that different phases appear, such as SbO_2, SbO_4 and Sb_2O_3. The broad background, which results from amorphous material is also increased in the extremely oxidized sample compared to the reference. Hence, non-stoichiometric and amorphous antimony oxide seems to have formed, additionally.

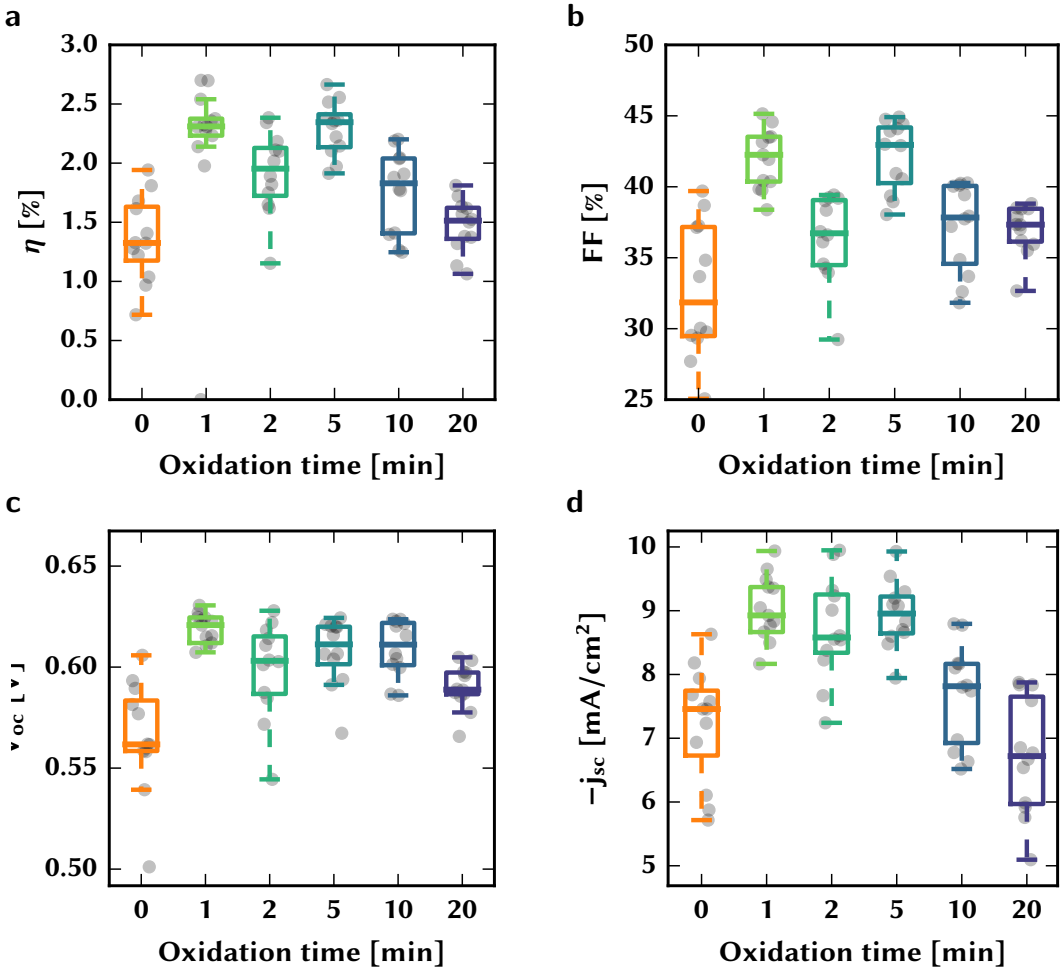

Figure S5: The photovoltaic parameters, (a) power conversion efficiency η, (b) fill factor FF, (c) open circuit voltage V_{oc} and (d) short-circuit current density j_{sc} for Sb_2S_3 sensitized solar cells for different post-heat treatment oxidation times at 200 °C.

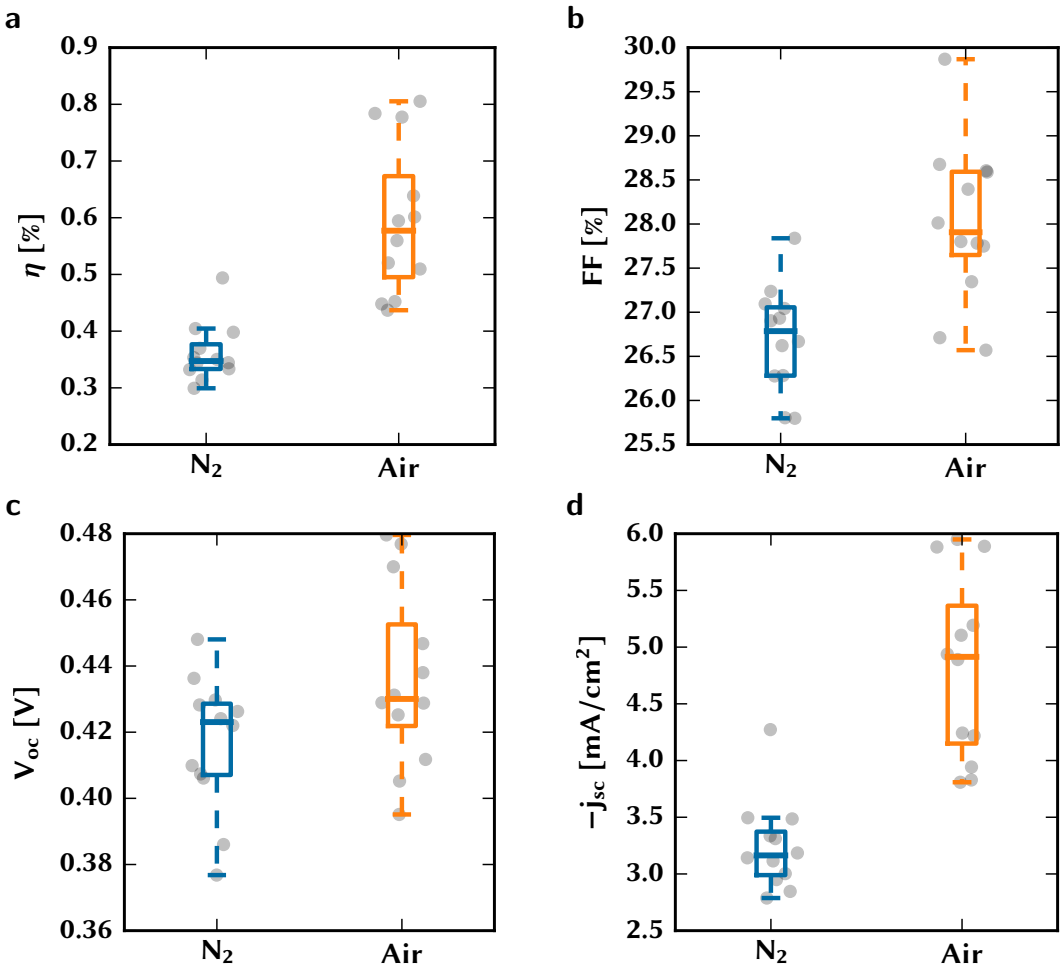

Figure S6: The photovoltaic parameters, (a) power conversion efficiency η, (b) fill factor FF, (c) open circuit voltage V_{oc} and (d) short-circuit current density j_{sc} for Sb_2S_3 sensitized solar cells heated in a nitrogen atmosphere at 200 °C for one minute (blue) and in air (orange).

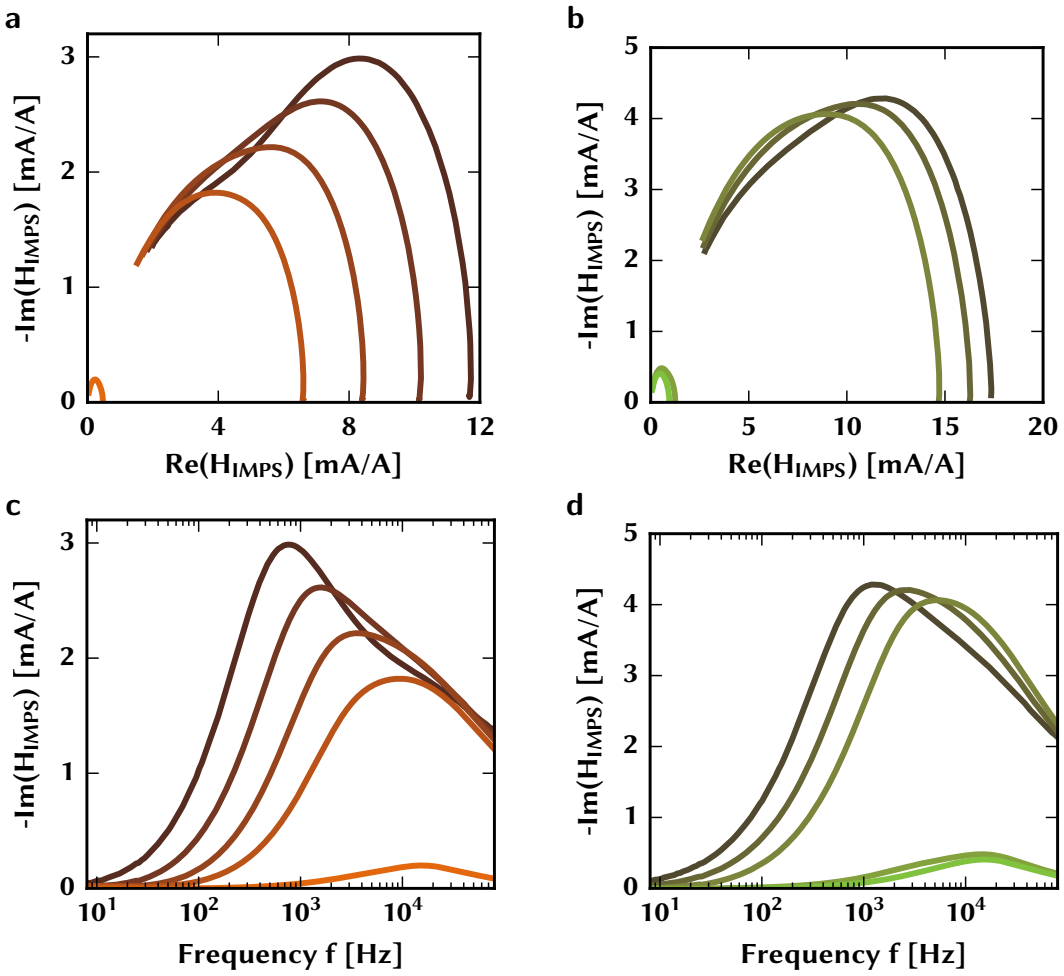

Figure S7: Intensity modulated photocurrent spectroscopy (IMPS) of non-oxidized and oxidized (1 min, 200 °C) solar cells. (a) Nyquist-plots for different levels of irradiance of a non-oxidized and (b) an oxidized device. (c) Bode-plots showing the same data as a function of frequency of a non-oxidized and (d) an oxidized solar cell.

Figure S7 shows Nyquist- (a and b) and Bode-type (c and d) plots for a device without oxidisation (orange colour scale, a and c) and one with a 1 min heat-treatment in air (green colour scale, b and d). Each plot shows the frequency dependent transfer function H_{IMPS}, which is defined by the used Autolab LED driver system as

$$H_{\mathrm{IMPS}} = \frac{\Delta I_{\mathrm{sc}}(t)}{\Delta I_{\mathrm{LED}}(t)}\,, \tag{2}$$

where $\Delta I_{\mathrm{sc}}(t)$ is the modulated short-circuit current response of the solar cell and $\Delta I_{\mathrm{LED}}(t)$ is the driving current of the intensity modulated LED illumination. For each device, the transfer function is measured for five different illumination base levels ($I_{\mathrm{LED}} = 38\,\mathrm{mA}, 75\,\mathrm{mA}, 150\,\mathrm{mA}, 300\,\mathrm{mA}, 600\,\mathrm{mA}$). The corresponding curves are shaded from dark orange/green (lowest illumination level) to bright orange/green (highest illumination level).

Table S1: Least-square fit parameters of a simple exponential function of the form $\tau_{\mathrm{tr}} = A_1 \exp(-B_1 \cdot I_{\mathrm{sc}}) + C_1$ and a logarithmic straight line $\ln(\tau_{\mathrm{rec}}) = -A_2 \cdot V_{\mathrm{oc}} + B_2$ to the data from IMPS and IMVS measurements.

	IMPS			IMVS	
	A_1 [ms]	B_1 $\left[\frac{1}{\mathrm{mA}}\right]$	C_1 [ms]	A_2 $\left[\frac{\ln(\mathrm{ms})}{\mathrm{V}}\right]$	B_2 [ln(ms)]
0 min	0.4601 ± 0.0335	17.924 ± 1.405	0.0128 ± 0.0036	21.088 ± 1.790	9.185 ± 1.012
1 min	0.2529 ± 0.0219	11.844 ± 1.176	0.0112 ± 0.0026	24.631 ± 1.510	12.722 ± 0.961

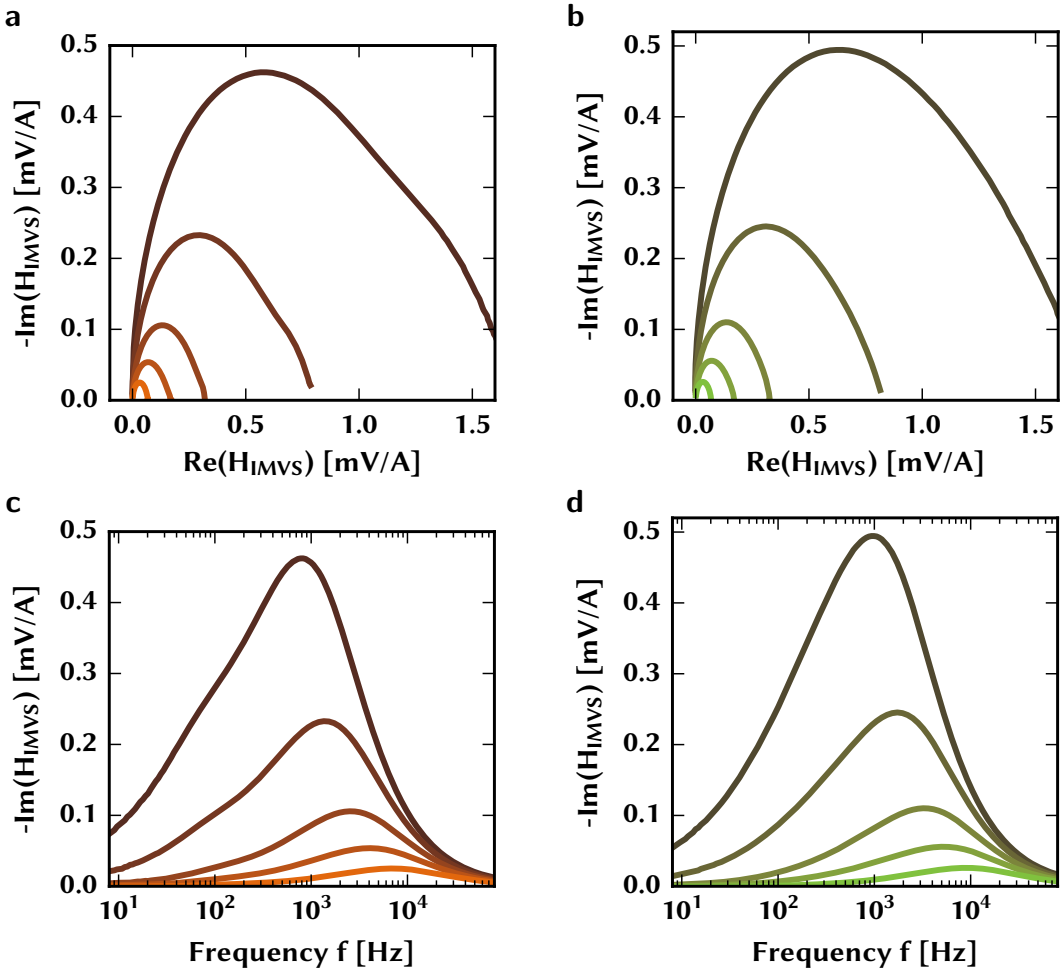

Figure S8: Intensity modulated photovoltage spectroscopy (IMVS) of non-oxidized and oxidized (1 min, 200 °C) solar cells. (a) Nyquist-plots for different levels of irradiance of a non-oxidized and (b) an oxidized device. (c) Bode-plots showing the same data as a function of frequency of a non-oxidized and (d) an oxidized solar cell.

Equivalently, the transfer function for IMVS H_{IMPS} is defined as

$$H_{\mathrm{IMPS}} = \frac{\Delta V_{\mathrm{oc}}(t)}{\Delta I_{\mathrm{LED}}(t)}\,, \tag{3}$$

where $\Delta V_{\mathrm{oc}}(t)$ is the modulated open-circuit voltage response of the photovoltaic device. Nyquist- and Bode-graph for the IMVS measurements are shown in Figure S8. The characteristic frequency can be easily determined from the Bode-plots (Figure S8 c and d) for the five different illumination irradiance levels by finding the frequency at which the imaginary part of the transfer function becomes minimal. Note that all plots show the negative imaginary part $-\mathrm{Im}(H_{\mathrm{IMPS/IMVS}})$.